

Optimization of ${}^6\text{He}$ production using W or Ta converter surrounded by BeO target assembly

N. Thiollière, J.C. David, V. Blideanu, D. Doré, B. Rapp, D. Ridikas

CEA Saclay, DSM/DAPNIA, 91191 Gif-sur-Yvette, France

1. Introduction

In this paper we describe the optimization work to produce ${}^6\text{He}$ beam within the EURISOL DS project [EDS]. The Monte Carlo code MCNPX [MCNP] is used for this purpose. The double stage target configuration, based on W converter and surrounded by BeO envelope as initially proposed by CERN [TS1] (see Figure 1), was further optimized with the goal to reach the production of $\sim 2 \cdot 10^{14}$ atoms/s in target. This intensity is required to satisfy the Beta-Beam needs [BB].

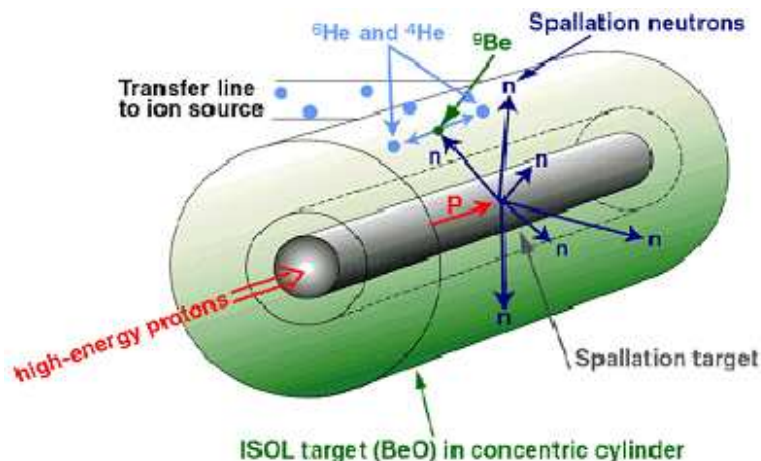


Figure 1: Two stage target for ${}^6\text{He}$ production [TS1].

In the following part, we study energy loss and neutron flux for a fixed system. First, energy loss gives information on thermal capacities of such a system. Then, neutron flux study, for a fixed geometry described below, allows determining a number of important parameters that can be modified in order to optimize the ${}^6\text{He}$ production. Finally, last paragraph details a number of promising ${}^6\text{He}$ production configurations.

2. Basic design parameters

We start our optimization study with the following initial assumptions. 1 GeV protons interact with the cylindrical target converter made of heavy metal as W or Ta (with the density of 19.35 g/cm^3 and 16.5 g/cm^3 respectively) to produce energetic neutrons. The primary beam power available is 100 kW and the beam has got a Gaussian distribution with

$\sigma = 6$ mm. Secondary neutrons interact with the surrounding envelope made of BeO and via the $n+{}^9\text{Be} \rightarrow {}^4\text{He}+{}^6\text{He}$ reaction produce ${}^6\text{He}$ ions. The reaction threshold is around 0.6 MeV. The production target density is $\rho = 1.806$ g/cm³.

The 2D geometry cuts of the ${}^6\text{He}$ production target are presented in Figure 2. Note that the proton beam axis coincides with z axis. This geometry configuration also contains a thin Ta container, where BeO is placed. First calculations are then made with a 1.5 cm radius tungsten/tantalum converter and a 2 cm thickness BeO target.

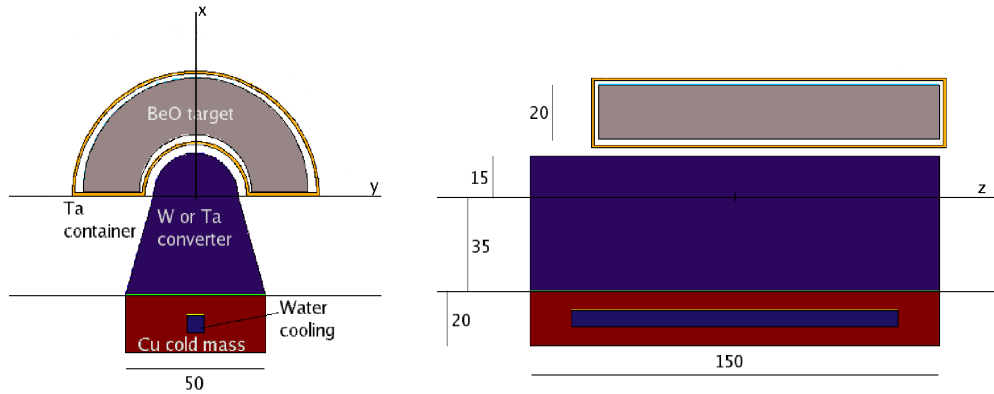


Figure 2: Initial geometry model within the MCNPX code. All dimensions are given in mm.

2.1. Proton beam description

The proton beam, parallel to z axis, has got a Gaussian profile with $\sigma = 6$ mm and generated automatically with the MCNPX code using σ_x and σ_y parameterization. A cross check of this description is presented in Figure 3, what proves that the incident beam is well-defined.

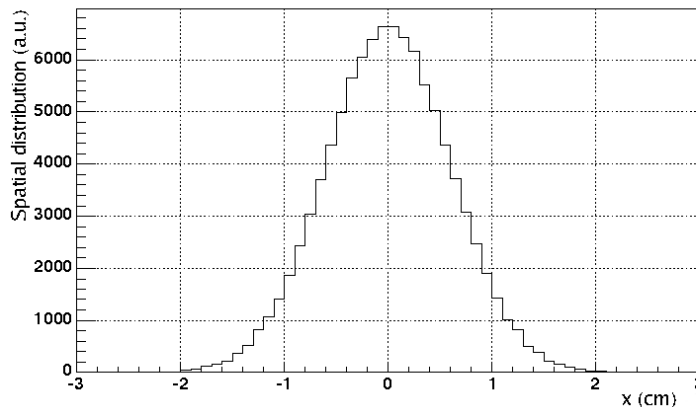


Figure 3: Spatial distribution of the incident proton beam on the input target surface.

2.2. Energy loss

The total energy loss in the entire target geometry, segmented into small volume elements, is calculated using energy loss mesh tallies as defined within MCNPX [MCNP]. Figure 4 shows the total energy loss distribution as a function of (x, y) coordinates and integrated over

the entire thickness of the target, i.e. integral along z direction (compare Figure 2 - on the left and Figure 4).

It is clear that the integration over (x, y) coordinates gives the total energy deposited in the system. For 1 GeV incident protons we obtain 368 MeV/p and 337 MeV/p for W and Ta converters (see Figure 2). In other words, only $\sim 35\%$ of the incident proton energy is deposited in the target. Note that $\sim 90\%$ of this quantity is deposited in the target converter, i.e. the production BeO target is nearly fully decoupled from the primary beam in terms of the energy deposition.

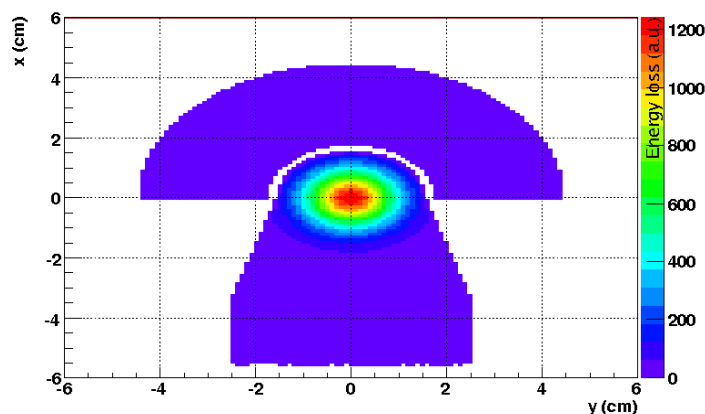


Figure 4: Simulation of the energy loss for tungsten converter.

Finally, the total energy deposition as a function of target thickness (z coordinate) in the case of a small $dx dy$ surface for four (x, y) chosen values is given in Figure 5. Those spectra show that the converter target length seems to be already optimized, i.e. most of the reactions take place within the 15 cm thickness and the 3 cm diameter. As it will be shown below, this conclusion will be confirmed by the neutron production.

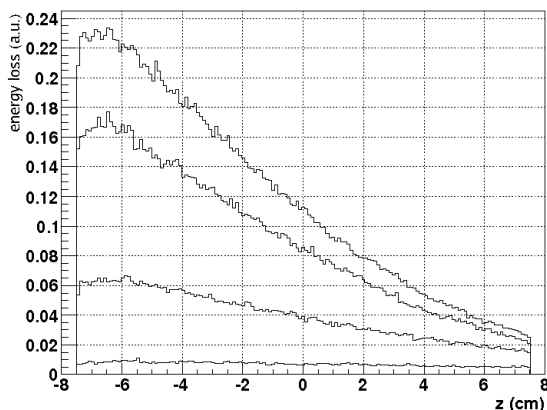


Figure 5: Total energy loss in the spallation cylinder according to z axis for $(x,y)=(0,0)$; $(x,y)=(0,0.5)$; $(x,y)=(0,1)$ and $(x,y)=(0,1.5)$ respectively for top to bottom spectra.

2.3. Neutron flux as a function of position

In order to observe neutron flux variations in the geometry, we plot in Figure 6 the neutron flux as a function of z coordinate for $y = 0$ and for several x -values. Those values have been

chosen to represent the centre of the converter ($x = 0$ cm), the border of the converter ($x = 1.5$ cm), the lower ($x = 2.15$ cm) and the upper ($x = 4.15$) limits of the BeO target.

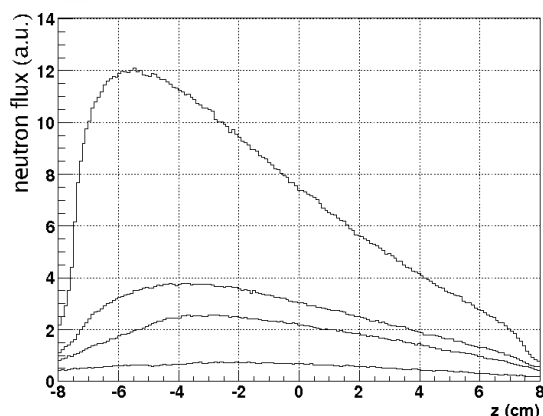


Figure 6: Neutron flux in arbitrary units versus z-axis for 4 dx dy area channels with positions (x,y) equal to (0,0), (1.5,0), (2.15,0) and (4.15,0) respectively from top to bottom.

Those spectra show that neutron flux at the z-limits of the system decreases to low values, what shows that there is no need for a longer converter.

2.4. Neutron flux versus energy

Energetic neutron flux is an important observable because it is directly related to the ${}^6\text{He}$ production. The neutron flux, calculated inside the BeO target volume, has a typical evaporation spectrum, characterised by high energy protons interacting with heavy mass targets. In addition, we observe (cf Figure 7) the “anti-resonance” on BeO target spectra due to elastic resonance scattering on ${}^9\text{Be}$ at $E_n = 0.62$ MeV and $E_n = 2.72$ MeV, and on ${}^{16}\text{O}$ at $E_n = 0.43$ MeV and $E_n = 0.99$ MeV.

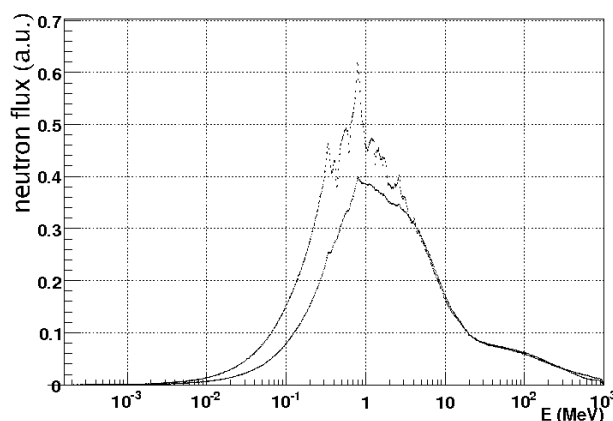


Figure 7: Comparison of neutron energy spectra in arbitrary units in the BeO target (upper line) and in the converter (bottom line).

Figure 7 shows that the neutron spectrum (in the BeO target) is peaked between ~ 0.1 MeV and ~ 10 MeV with the average neutron energy ~ 1 MeV. This neutron flux has to be optimized to maximize the ${}^6\text{He}$ production by keeping in mind the shape of the ${}^9\text{Be}(n,\alpha){}^6\text{He}$ reaction cross section as shown in Figure 8 (extracted from ENDF.B-VI.0 data base [ENDF]).

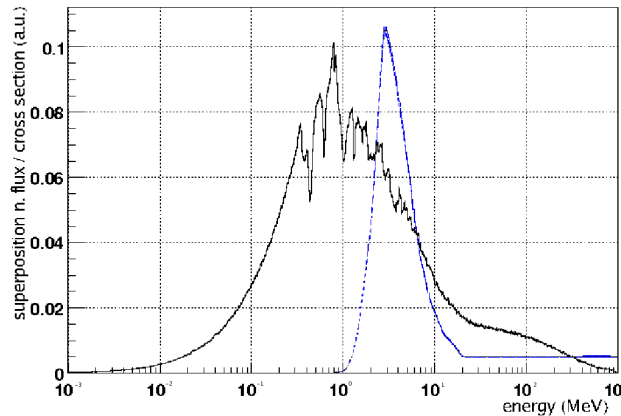


Figure 8: Neutron flux (black line) and renormalized ${}^6\text{He}$ production cross section (blue line) compared as a function of neutron energy.

It seems that the neutron flux is far from optimal in order to maximise the ${}^6\text{He}$ production. It is clear that a neutron flux distribution shift to higher energies could still increase considerably the ion production.

2.5. ${}^6\text{He}$ production in the reference configuration

For the initial geometry described above the only remaining variable is the choice of the physics model within MCNPX. Table 1 shows the dependence of the ${}^6\text{He}$ production for several physics models in the Tungsten and Tantalum converter case. As a matter of fact all models show comparable predictions (within 15%). This result is understandable, since it is well known that all models are rather accurate in predicting neutron production from spallation reactions [SL]. We note separately that a Tungsten converter is more efficient than a Tantalum converter.

	INC / EVA	${}^6\text{He}$ (% / inc. p.)	${}^6\text{He}$ ($\times 10^{13}/\text{s}$)
W	Bertini / Dresner	3.42 ± 0.01	2.13 ± 0.01
	Bertini / ABLA	3.99 ± 0.02	2.49 ± 0.02
	ISABEL / ABLA	3.50 ± 0.01	2.18 ± 0.01
	INCL4 / ABLA	3.28 ± 0.01	2.05 ± 0.01
Ta	Bertini / Dresner	3.29 ± 0.01	2.06 ± 0.01
	Bertini / ABLA	3.84 ± 0.02	2.40 ± 0.02
	ISABEL / ABLA	3.30 ± 0.01	2.06 ± 0.01
	INCL4 / ABLA	3.11 ± 0.01	1.94 ± 0.01

Table 1: Model dependence of the ${}^6\text{He}$ production for the reference geometry (see text for details), for the W and Ta converters. The statistical error in all cases was less than 0.5%. The normalization is in (% per incident p) in the 1st column and for 100 kW (1GeV; 100 μA) primary proton beam in the 2nd column.

2.6. Intermediate summary

The goal of the above work was to study the ${}^6\text{He}$ production starting with the earlier proposed reference configuration. The obtained result is still by one order of magnitude lower than the desired in-target production rate, i.e. $2 \cdot 10^{14}$ atoms/s (compared to Table 1). The possible optimization parameters in order to gain a factor of 10 in ${}^6\text{He}$ production are treated in the next paragraph. First, we discuss on theoretical assumptions in order to identify accessible

ways to increase the production rate. Then, we continue with some independent system modifications around the initial configuration. Finally, a combination of all independent modifications is made, what leads to the optimized ${}^6\text{He}$ production system.

3. Geometrical modification

3.1. Theoretical features

Analytic expression of ${}^6\text{He}$ production can be written on the following form:

$$\tau({}^6\text{He}) = N_{\text{Be}} \int_E \int_V (\sigma_{(n,\alpha)}(E_n) \phi_n(E_n, \vec{r})) dV dE_n, \quad (1)$$

where $\tau({}^6\text{He})$ represents ${}^6\text{He}$ production rate (atom/s) in the entire BeO target. N_{Be} is the ${}^9\text{Be}$ atom density (atoms/cm³), dV , a BeO target infinitesimal volume, $\sigma_{(n,\alpha)}(E_n)$ represents ${}^9\text{Be}(n,\alpha){}^6\text{He}$ reaction cross section (barns). Finally, neutron flux with energy between E_n and E_n+dE_n is represented by ϕ_n (n/cm²/s/MeV). It is evident that to optimize ${}^6\text{He}$ production consists to maximize Eq.(1), what can be done by three different ways when analyzing Figure 8.

1. The shift of neutron flux to higher energies. In brief, this can be achieved in part by an increase of the incident proton energy, since this would lead to higher excitation energies of the target nucleus. Consequently, the increased excitation energy would be shared between the number of neutrons (and other secondary particles) created and their kinetic energy.
2. The slowing down of fast neutrons ($E > 20$ MeV): keeping in mind Figure 8 one can see that neutron flux with energy between 20 MeV and 1 GeV, which has no effect for the isotope production, might still be important. One could imagine to insert a reflector in order to recover and to slow-down those neutrons. On the other hand, it appears to be very difficult to slow-down fast neutrons without modifying the energy of already “optimized” neutrons ($E \sim 3$ MeV) for ${}^6\text{He}$ production.
3. The increase of the absolute neutron flux:
 - Note that in this case the choice of the converter target material is very important. First of all, the high neutron production imposes a high nuclear mass and density. In addition, a material with a high melting point is desired. So tungsten, with a density $\rho = 19.4$ g/cm³ and a melting point temperature $T = 3410^\circ\text{C}$ appears to be an optimized choice.
 - Increase in incident proton energy also should be examined. This was already mentioned in the above option (1). However, one should not forget that increase in neutron production per incident proton energy (or incident beam power) reaches saturation for energies higher than 1 GeV.
 - Another way to increase absolute neutron flux consists to add a reflector in the target geometry. Indeed, neutron mean free path λ in BeO target is close to 4 cm associated with total cross section for 4 MeV neutrons, while $\lambda \sim 230$ cm for ${}^9\text{Be}(n,\alpha)$ reaction. That implies that few neutrons interact in BeO target so it is possible to increase neutron flux by adding a reflector. What implies also that the BeO geometry (i.e. its position, length or radius) is an obvious parameter to modify in order to optimize the production of ${}^6\text{He}$.

All those modifications are independently tested in next paragraphs. We used is INCL4-ABLA physics models within MCNPX for further optimisation study.

3.2. Converter size

In this paragraph we determine the optimal converter radius R and length L . Numerical simulations with a Tungsten converter have been done for a fixed length ($L=20$ cm) and for several converter radii. For each radius, the primary beam profile is defined by Gaussian distribution with parameter $\sigma = R/3$ in order to redistribute the incident proton flux on the target. Absolute number of emitted neutrons with energy between 3 MeV and 5 MeV (i.e. the energy region which includes important neutrons for ${}^6\text{He}$ production) has been extracted, what is presented in Figure 9. It is clear that the converter radius should be bigger than 1 cm. On the other hand, a 1 cm radius converter results in not acceptable thermal hot point due to high incident protons concentration [TS2]. From this point of view, a converter radius of 1.5 cm leads to a favourable thermal response.

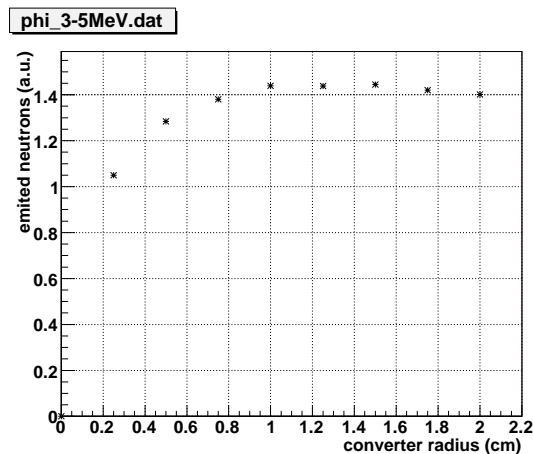


Figure 8: Absolute number of emitted neutrons (between 3 and 5 MeV) versus converter radius.

For the converter length optimization, we extract absolute number of emitted neutrons, for $R = 1.5$ cm, versus converter length (see Figure 9). We conclude that neutron emission saturates for the converter length close to 25 cm.

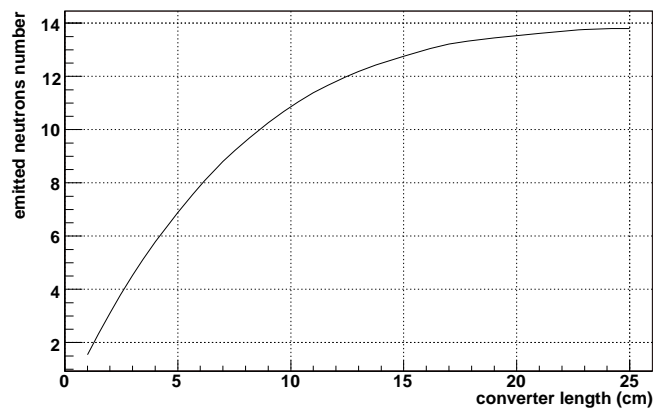


Figure 9: Emitted neutrons versus converter length for radius 1.5 cm.

This 1st optimization step, what includes the length and radius of converter, leads to the ${}^6\text{He}$ reaction rate $\tau = 4.22\% \text{ } {}^6\text{He} / \text{inc. } p$, i.e. a gain factor of 1.2.

3.3. BeO target position and dimension

In this paragraph, we extract and visualise the spatial neutron flux distribution in order to optimize the BeO target geometry. We start with the initial converter configuration (L=15 cm and R=1.5 cm), where the neutron flux is calculated within a mesh tally and represented as a function of (z,x) on Figure 10. The converter limits are defined by $-7.5 < z < 7.5$ and $0 < x < 1.5$.

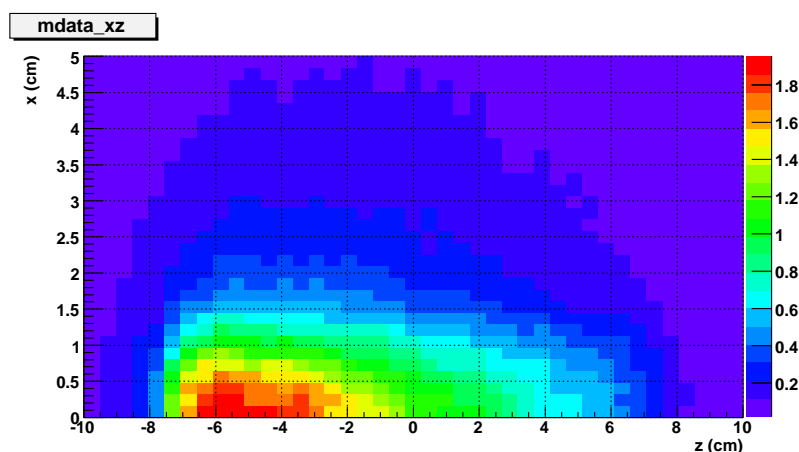


Figure 10: Neutron flux versus x and z -dimensions in the geometry that includes only cylinder of W.

At the BeO target lower limit (i.e. $x \sim 1.85$ cm), we obtain the maximum value ϕ_{\max} of the neutron flux (for $z \sim -5$ cm). Then, we select xz coordinates for which neutron flux ϕ fulfils the following arbitrary condition $\phi > 0.25 \phi_{\max}$. Figure 611, shows then the optimized BeO target shape.

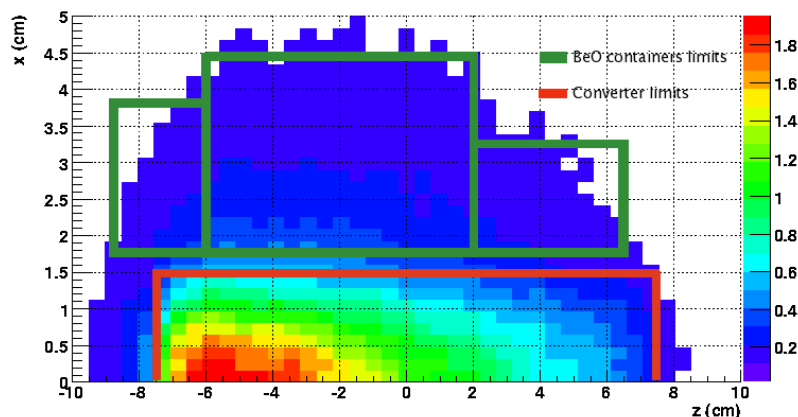


Figure 61: Neutron flux selection versus x and z -dimension superposed with converter and BeO containers limits.

In order to adjust the BeO target shape (see Figure 12), we divided it into three independent containers, where each of them has an exterior radius in accordance to the limits given by Figure 11.

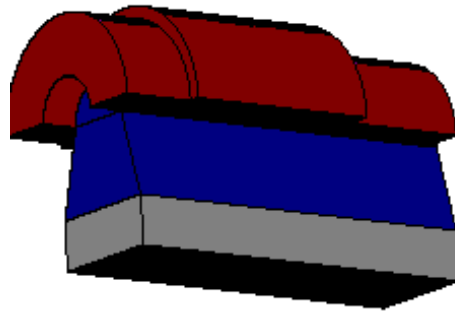


Figure 12: *BeO target composed by three containers in the MCNPX geometry representation .*

Numerical computation with this new geometry leads to a ${}^6\text{He}$ production rate $\tau=4.48\% \text{ } {}^6\text{He}/\text{inc. } p$, i.e. a gain factor of 1.3.

Another tested modification, consists to increase the volume of the BeO target as shown in Figure 13 (compared to Figure 12). This last geometry modification results in the reaction rate $\tau=5.13\% \text{ } {}^6\text{He}/\text{inc. } p$ (1.5 gain factor).

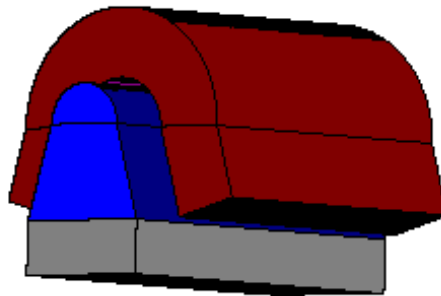


Figure 13: *Modified BeO target geometry by increasing its volume.*

3.4. Influence of reflector

As we already discussed in paragraph 3.1., it seems that most of the neutrons cross the BeO target without interaction. A reflector disposed around the entire system should then increase neutron flux in the target. This reflector must satisfy the following criteria:

- The mean free path for the scattering process given by $\lambda = A/(N_a \rho \sigma_s)$ should be minimum in order to limit the scattering solid angle towards the BeO target. This implies a high scattering cross section σ_s and a low A/ρ value.
- A low absorption cross section in order to minimize neutron loss.

In this context, we test then three reflectors composed of light elements such as water (H_2O), heavy water (D_2O) and graphite (C) and three heavy-medium reflectors, iron (Fe), tungsten (W) and lead (Pb). The mean free path for neutron energies close to few MeV in such a

medium is of the order of few centimetres. So, we have enclosed the system by a 20 cm thick reflector, what resulted in following ${}^6\text{He}$ production rates as a function of reflector material:

$$\tau(\text{Pb})=4.00\% \text{ } {}^6\text{He} / \text{inc. } p$$

$$\tau(\text{W})=3.76\% \text{ } {}^6\text{He} / \text{inc. } p$$

$$\tau(\text{Fe})=3.74\% \text{ } {}^6\text{He} / \text{inc. } p$$

$$\tau(\text{C})=3.72\% \text{ } {}^6\text{He} / \text{inc. } p$$

$$\tau(\text{D}_2\text{O}) = 3.48\% \text{ } {}^6\text{He} / \text{inc. } p$$

$$\tau(\text{H}_2\text{O}) = 3.47\% \text{ } {}^6\text{He} / \text{inc. } p$$

In brief, lead (Pb) appears to be the most efficient with a 1.17 gain factor in ${}^6\text{He}$ production compare to the baseline system.

3.5. Incident proton beam

In this paragraph, we examine the influence of proton beam energy for the production of ${}^6\text{He}$. In order to adjust converter length, we compare total energy loss and neutron flux for 1 GeV and 2 GeV proton beams (see Figure 14).

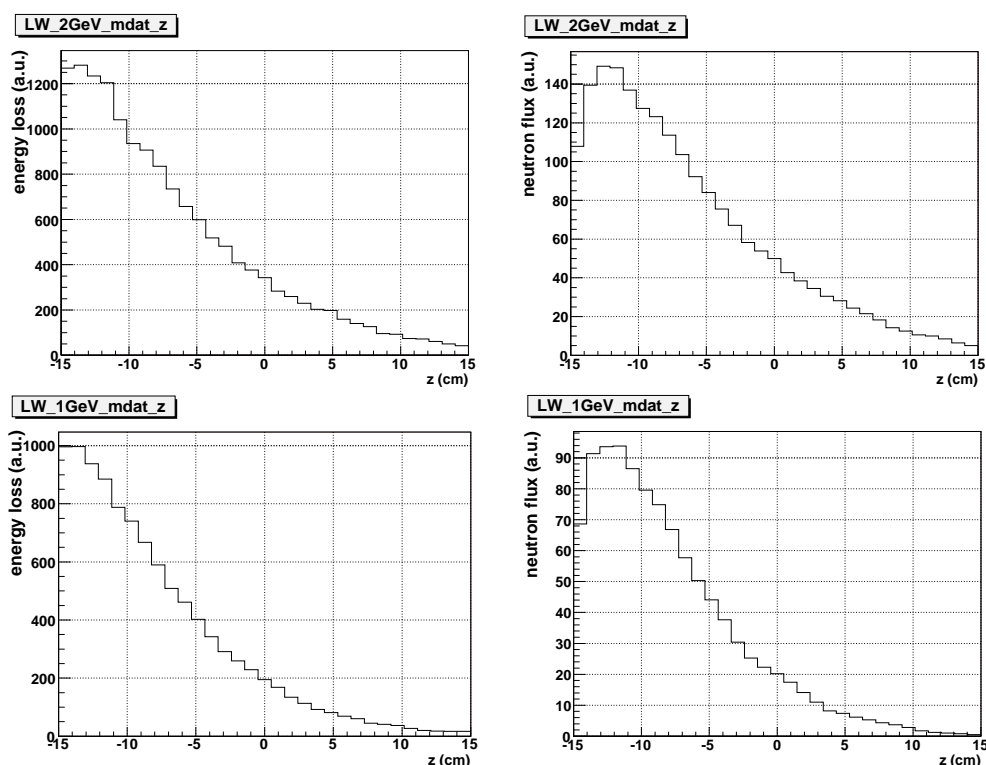


Figure 14: Total energy loss and neutron flux for 1 GeV (lower part) and 2 GeV (upper part) proton beam.

Let us consider the initial converter length of $L = 15$ cm for 1 GeV protons. In the case of 2 GeV protons we estimate that the “equivalent” length would be between 20 and 24 cm. The “equivalence” was established in terms of comparable energy deposition and neutron production. Finally, with the 24 cm long converter and adjusted BeO target length we obtain that the ${}^6\text{He}$ production is $\tau=8.43\% \text{ } {}^6\text{He} / \text{inc. } p$ (gain of 2.5).

3.6. Combination of independent modifications

Combining all described independent modifications we obtain an optimized geometry for 2 GeV protons (see Figure 15) leading to the ${}^6\text{He}$ production $\tau=18.31\% {}^6\text{He}/inc.p$

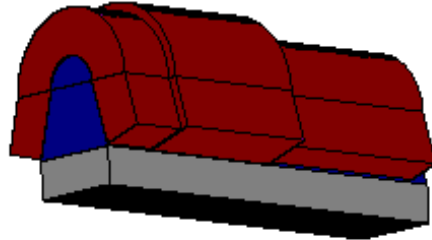


Figure 15: The optimized (in terms of in target yields) target geometry to produce ${}^6\text{He}$ beams.

Assuming that this configuration can function at 200 kW (2 GeV; 100 μA) power we obtain the following in target production rate $\tau=1.14\cdot 10^{14} {}^6\text{He}/s$.

One must note that this optimized configuration must be examined as long as its thermal conditions are acceptable. Indeed, the converter is closely surrounded by BeO target, what limits heat evacuation. Such a study will be performed at CERN in the near future [TS2].

4. Conclusion

In this paper we studied the ${}^6\text{He}$ production in the two-stage system (neutron converter – ion production targets) for the EURISOL-DS needs. Following the baseline parameters [TS1], we worked in more detail on thermal and neutron flux observables for a system composed of a Tungsten or Tantalum converter, surrounded by a BeO target. Incident proton beam has been fixed to 1 GeV with a 100 kW power. We confirmed that this initial configuration does not allow reaching the desired in target ${}^6\text{He}$ production rate, i.e. we obtained $2\cdot 10^{13}$ ions/s compared to $2\cdot 10^{14}$ ions/s.

A number of geometry, material and incident beam parameters were optimized with the goal to increase the production rate by a factor of 10. For this purpose we used the MCNPX code. We show that a gain factor of 5 compared to the initial reference configuration can be obtained, i.e. the final ${}^6\text{He}$ production rate is $\sim 1\cdot 10^{14} {}^6\text{He}/s$.

We add that further increase in production of ${}^6\text{He}$ ions could be achieved “simply” by increasing the external BeO target radius, i.e. by increasing the volume of production target. On the other hand, such a geometry modification would certainly induce ${}^6\text{He}$ on-line extraction losses, i.e. the final increase in available ${}^6\text{He}$ ion beam is not guaranteed. Additional studies on the extraction efficiency should be done shortly.

5. Acknowledgments

We would like to thank T. Stora (CERN) for fruitful discussions in preparing this manuscript.

We acknowledge the financial support of the EC under the FP6 "Research Infrastructure Action - Structuring the European Research Area" EURISOL DS Project; Contract No. 515768 RIDS; www.eurisol.org. The EC is not liable for any use that may be made of the information contained herein.

6. References

- [EDS] EURISOL DESIGN STUDY (web site: <http://www.eurisol.org/site01/index.php>).
- [MCNP] Denise B. Pelowitz, MCNPX user's manual, version 2.5.0, April 2005.
- [TS1] T. Stora, E. Bouquerel, J. Lettry. W converter BeO target prototype for ${}^6\text{He}$ production - version 1. EURISOL-DS-TASK 3; "direct target" contribution to the "beta beams" task.
- [BB] M. Lindroos, The Technical challenges of Beta-beams, Conference (12/2005)
- [SL] S. Leray et al., Phys. Rev. C65, 044621 (2002).
- [WFW] W.F. Weisskopf, Phys. Rev. 52 (1937) 295.
- [SV] Stéphane Vuillier. Thèse de doctorat. Simulation pour la transmutation des déchets par réacteur hybrides. CENBG (06/1998).
- [ENDF] NNDC Online Data service, telnet.nndc.bnl.gov.
- [TS2] T. Stora; private communication (2006).